Nonlinear Scattering and Absorption Effects in Size-Selected Diphenylpolyynes

ARTICLE *in* THE JOURNAL OF PHYSICAL CHEMISTRY C · DECEMBER 2014

Impact Factor: 4.77 · DOI: 10.1021/jp509666x

9 AUTHORS, INCLUDING:

Luisa D'urso
University of Catania
40 PUBLICATIONS **384** CITATIONS
SEE PROFILE

Giuseppe Compagnini
University of Catania
176 PUBLICATIONS **2,689** CITATIONS
SEE PROFILE

O. Puglisi
University of Catania
117 PUBLICATIONS **1,637** CITATIONS
SEE PROFILE

Salvatore Patanè
Università degli Studi di Messina
102 PUBLICATIONS **882** CITATIONS
SEE PROFILE

THE JOURNAL OF PHYSICAL CHEMISTRY C

Article

pubs.acs.org/JPCC

Nonlinear Scattering and Absorption Effects in Size-Selected Diphenylpolyynes

E. Fazio,[†] L. D'Urso,*[,‡] G. Consiglio,[§] A. Giuffrida,[∥] G. Compagnini,[‡] O. Puglisi,[‡] S. Patanè,[†] F. Neri,[†] and G. Forte[⊥]

[†]Dipartimento di Fisica e di Scienze della Terra, Università di Messina, Viale F. Stagno d'Alcontres, 31 - 98166 Messina, Italy

[‡]Dipartimento di Scienze Chimiche, Università di Catania, Viale Andrea Doria 6, 95125 Catania, Italy

[§]Dipartimento di Ingegneria Industriale, Università di Catania, Viale Andrea Doria 6, 95125 Catania, Italy

[∥]Consiglio Nazionale delle Ricerche, Istituto di Biostrutture e Bioimmagini U.O.S. Catania, Via Gaifami 18, 95125 Catania, Italy

[⊥]Dipartimento di Scienze del Farmaco, Università di Catania, Viale Andrea Doria 6, 95125 Catania, Italy

Supporting Information

ABSTRACT: The nonlinear optical properties of monodispersed diphenylpolyynes with different chain length were studied by using a nanosecond pulsed laser excitation. A strong optical limiting response was detected at laser fluences above 0.35 J/cm^2. The nature of the nonlinear effect as a function of the number of carbon atoms in the linear chain was investigated by the Z-scan technique, determining the molecular second-order hyperpolarizability γ. An interesting coupling was found between the decrease of scattering phenomena and the alignment of longer carbon chains in the focus region. The effect of an external highly intense electric field, combined with a detailed density functional theory (DFT) investigation, has been invoked to explain molecular arrangement, polarizability, isomery, and scattering of diphenylpolyynes. The interesting findings derived from our investigations demonstrate that phenyl-end-capped polyynes could be very interesting for various optoelectronic applications.

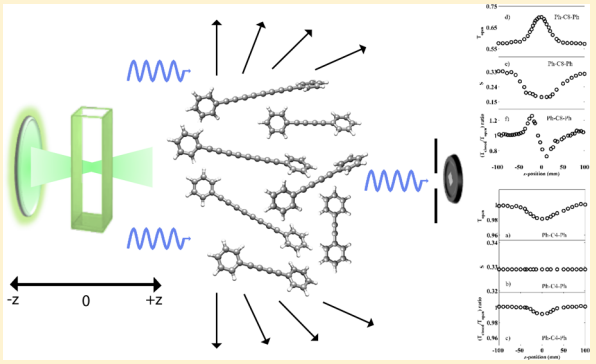

1. INTRODUCTION

Organic wires of atomic thickness have emerged as a new type of one-dimensional materials with remarkable molecular-scale functionality. They are prospected as the future of molecular optoelectronic devices, and they can usefully substitute the traditional inorganic semiconductors (e.g., Si, GaAs).[1] Between them, sp-hybridized carbon molecules exhibit some very unusual physical and optoelectronic properties due to the delocalized π electron states present along their chain.[1−5]

In these molecules, the HOMO−LUMO gap not only is strongly influenced by the number of sp carbon atoms in the chain but also, as very recently reported in literature, depends on the nature of the end-capping group of the linear carbon chains (LCCs).[2] In these resulting structures, the nearly 1 nm long LCCs can be torsionally stiff, due to the broken axial symmetry with staggered π bonds, thus inducing a change of linear optical properties. Particularly the stiffness, emerging at the electronic structure level, can lead to a tuning of the band-gap from 2.6 to 4.7 eV under a 10% strain.[2]

At present, a limitation in technological applications for sp-hybridized carbon wires is their chemical stability in a wide range of working conditions. A crucial aspect in polyyne chemistry is connected to the high reactivity of adjacent carbon chains. Most of the experiments have revealed interchain interaction and a cross-linking degradation into more stable sp^2. These reactions are strongly enhanced by the high concentration, when dispersed in liquid, and by temperature higher than RT or light exposure.[6−9] Moreover the molecular structure in the excited states of polyyne is complicated because of their dramatic isomerization. One way to hinder the degradation is the connection of the carbon molecular wire ends to metal nanoparticles[10] by means of electrostatic interaction, but the instauration of long-range interacting forces, instead of covalent bonds, makes these hybrid systems still unstable for optoelectronic application on a large scale. Another method was their insertion into solid-phase materials as carbon nanotubes[11,12] or by the simultaneous complexation with α-cyclodextrin rotaxanes.[13] Cataldo et al. have shown, through UV−vis and FT-IR studies, that LCC degradation is remarkably inhibited when hydrogen terminations are substituted with an organic group.[14−17] Stable polydispersed diphenylpolyynes were synthesized and characterized by Cataldo et al. after HPLC separation.[15] Diphenylpolyynes are a suitable compound to perform spectroscopic studies on the excited states of linear

Received: September 24, 2014
Revised: November 13, 2014
Published: November 14, 2014

   dx.doi.org/10.1021/jp509666x | J. Phys. Chem. C 2014, 118, 28812−28819

sp-hybridized carbon chains because the phenyl terminations reduce the isomerization and the chemical reactivity.[18] Ravagnan et al.[19] carried out a study on the correlation between axial torsion and electronic transitions in sp^2-terminated carbon chains, and recently a theoretical investigation of the geometry of ground and excited states of a series of diphenyl butadiynyl fluorophores has been accomplished by Pati et al.[20]

In this context, we demonstrate how the optical nonlinear response of monodispersed diphenylpolyynes is affected by their end-capping groups and chain length. In a previous work[21] we reported the nonlinear optical behavior of hydrogen-terminated LCCs synthesized by laser-generated plasmas in different solvents. We highlighted that both the solvents and the chain length distribution have a driving role in the optical response; a reverse saturable absorption (RSA) and saturable absorption (SA) behavior were observed in LCCs produced in polar and apolar solvents, respectively. The effect of solvent polarity and acidity was taken into account to explain the nature of the optical limiting behavior.

In this work monodispersed diphenylpolyynes were synthesized by palladium-catalyzed self-coupling reaction of terminal alkyne.[22] An extensive theoretical and experimental study of the optical properties of monodispersed linear carbon chains is reported. An interesting coupling between the nature of the optical limiting response, the molecule alignment under a polarized high-power laser excitation, and the carbon chain length was found. We theoretically investigate the torsional/orientational and polarizability effects on the electronic structure of diphenylpolyynes placed in planar geometries, also under an external highly intense electric field. A relevant technological aspect is that the longer-chain structures are stable, maintaining an effective optical response, both at rest and under high light flux.

2. EXPERIMENTAL SECTION

Monodispersed symmetrical polyynes (Ph-C4-Ph and Ph-C8-Ph), used in our experiments, were synthesized via palladium-catalyzed cross-coupling of 1-alkynes and characterized by an ion trap electrospray mass spectrometer (see Supporting Information, Synthesis and characterization of diphenylpolyynes paragraph for details).

Ph-C2-Ph was purchased by Sigma-Aldrich. Diphenyl polyynes (Ph-C2-Ph, Ph-C4-Ph, and Ph-C8-Ph) were dissolved in methanol at a concentration of 1×10^{-5} M. Henceforth, the monodispersed symmetrical polyynes were Ph-C2-Ph, Ph-C4-Ph, and Ph-C8-Ph. UV−vis optical transmission measurements were carried out using an UV−vis−NIR PerkinElmer spectrophotometer. The UV−vis optical absorption of fresh and 2 weeks old solution was measured in the range 190−1100 nm. Absorption spectra were also recorded before and after the nonlinear optical limiting measurements.

The nonlinear optical properties have been determined by the Z-scan method[21] using a pulsed Nd:YAG laser (wavelength 532 nm, 5 ns pulse duration, 10 Hz repetition rate). The incident laser beam was divided by a beamsplitter: the reflected part was taken as the laser beam correction (input), and the transmitted one (output) was focused, with a 300 mm focusing lens, into a 1 cm length quartz cuvette. A second detector, mounted at 90° with respect to the laser propagation direction, allows us to collect simultaneously the scattered light (point to point along z) with a dual channel energy meter. The optical limiting measurements were carried out by moving the sample along the axis of the incident beam (z direction) with respect to the focal point and keeping constant the laser pulse energy. To determine the nonlinear refractive index n_2 and the nonlinear absorption coefficient β, the measurements were taken in both closed and open aperture configurations.[23] In the closed aperture configuration a finite aperture (d = 500 μm) was placed at 300 mm from the focal point. All the measurements were carried out with a laser fluence of 1.5 J/cm^2 in the focal region.

3. MATERIAL AND METHODS (DFT)

The equilibrium geometry of PhC_nPh (n = 2, 4, 8) was calculated in methanol using the hybrid functional PBE0, which uses 25% exchange and 75% correlation weighting,[24−26] and the 6-311+** basis set.[27,28] In order to evaluate the rigidity of the aromatic group with respect to the linear chain, for each compound we have considered four isomers characterized by different dihedral angle between aromatic end groups (see Figure 4). The values chosen for the angles were, respectively, 0, 30, 60, and 90° and were kept fixed during the optimization. Henceforth, consistent with the general formula reported above, the isomers of each compound will be named by using the following nomenclature: C-n-value of the dihedral angle. So, as an example, the compound C-4-30 will indicate the isomer of Ph-C4-Ph with an aromatic group forming a dihedral angle of 30° with respect to the CC chain. In order to evaluate the solvent effect the conductor-like polarizable continuum model (CPCM)[29−31] was adopted. Time-dependent DFT calculations were used to calculate the UV−vis spectra.[32−34] The UV−vis spectra were simulated via a configuration interaction that involves 25 excited states starting from the optimized geometries. Finally the molecular polarizability tensor, α, is calculated as the derivative of the induced molecular dipole moment $\boldsymbol{\mu}_p$ with respect to an external electric field $\mathbf{E}_q$ whose frequency is set to the experimental value at which the Z-scan measurements were carried out. In atomic units α yields volume units; therefore, we will refer to it as volume polarizability.

4. RESULTS AND DISCUSSION

4.1. Z-Scan Measurements. In Figure 1, the limiting curves obtained for the shorter (Ph-C2-Ph, Ph-C4-Ph) and longer (Ph-C8-Ph) carbon chains in methanol solutions, when repetitively irradiated by a visible laser pulse lasting a

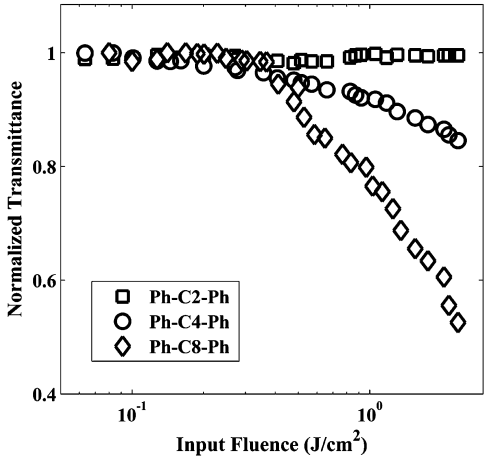

Figure 1. Nonlinear optical limiting performance of the carbon chains toward 532 nm laser light input fluence.

dx.doi.org/10.1021/jp509666x | J. Phys. Chem. C 2014, 118, 28812−28819

few nanoseconds, are depicted. The transmittance is the ratio between the output and the input (point to point along z) beam intensities. Then, the so-obtained values are normalized to the ones acquired outside the region of nonlinearity. We observe that the transmittance begins to decrease at a fluence of 0.35 J/cm^2. This value, corresponding to the onset of the optical limiting threshold, is found to be comparable to that reported for carbon nanotubes.[35,36] The transmittance is halved at around 2 J/cm^2 only for the longer chains (Ph-C8-Ph), while for the shorter carbon chain (Ph-C4-Ph), the transmittance reaches nearly 1/2 of the initial value at around 12 J/cm^2 (not shown). No nonlinear response is observed for the Ph-C2-Ph chains in methanol, showing that the effect increases with the carbon chain length.

In order to determine the nature of the nonlinear mechanisms, the Z-scan measurements were carried out in both the open and closed aperture configurations, by measuring the real and imaginary part of the third-order susceptibility $\chi^{(3)}$, respectively. Hence, the normalized transmittance curves, reported as a function of the Z-scan position and analyzed using the procedure described by Bahae et al.,[23] allow us to distinguish the pure nonlinear absorption contribution from the refractive one. For this purpose, the refractive contribution to the nonlinearity is isolated from the absorption contribution by dividing the normalized transmittance, collected along the beam direction propagation and placing a pinhole before the detector (closed configuration), by the normalized transmittance when no aperture is present (open configuration).[23] In Figure 2 the

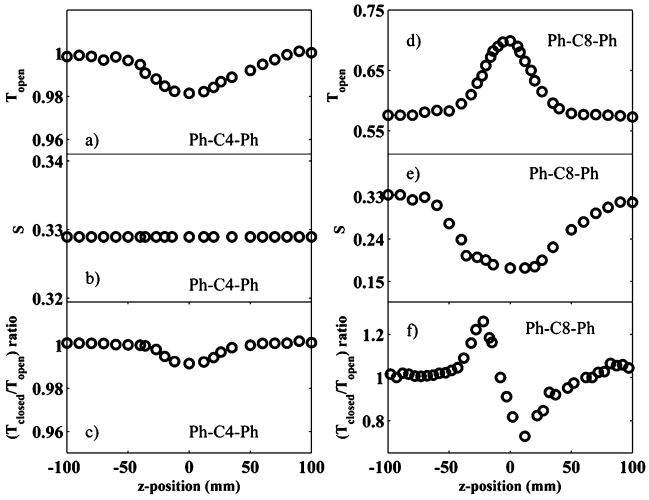

Figure 2. Transmittance T_{open} (a, d), 90° scattering (S) (b,e), and transmittance (T_{closed}/T_{open}) ratio (c,f) values as a function of the sample position z, for the Ph-C4-Ph and Ph-C8-Ph carbon chains.

transmittance and the scattering values as a function of the sample position "z" are reported.

The open transmittance curve of Ph-C4-Ph carbon chains shows a symmetrical minimum in the focus region (see Figure 2(a)). This behavior implies that the mechanism which mainly determines the optical limiting response of Ph-C4-Ph carbon chains is the nonlinear absorption mechanism (the dip is a feature characteristic of an RSA mechanism). The closed/open feature of Ph-C4-Ph carbon chains is similar to that obtained in the open aperture configuration, and no change in the 90° scattering signal was detected (see Figure 2(b) and Figure 2(c)). Thus, the contributions associated with the variation of the refractive index n_2 or to the scattering effects do not determine the nonlinear optical response.

For the Ph-C8-Ph carbon chains, the scattering signal decreases in the focus region, showing a dip that reaches a minimum value around 0.15, while the signal collected along the beam propagation direction (open configuration) is characterized by an increased transmittance symmetrical peak near the focus position (z = 0) (see Figure 2(d) and Figure 2(e)). Then, it is the reduced scattering contribution that affects the transmittance increase and, ultimately, the OL response of the Ph-C8-Ph carbon species. As will be reported in the next paragraphs (see DFT Calculations paragraph), the greater size of the Ph-C8-Ph molecules gives rise to the presence of several conformers as well as to a sensitive response to high power laser excitation in terms of photoinduced molecule orientation. As a result, the electric field of intense laser radiation will induce an instantaneous electric dipole which will tend to align the carbon chains. In particular, the Ph-C8-Ph molecules are forced to become parallel to the optical axis in the focus region, and in this configuration, their 90° scattering efficiency decreases, determining an increase of the forward transmittance. This behavior is in good agreement with the one reported by Hirofumi et al. for the alignment of neutral molecules in a strong laser field.[37]

Moreover, a similar behavior has been observed with regard to the effect of radiation torque and force on an optically trapped linear nanostructure.[38]

On the other hand, a prefocal transmittance maximum (peak) followed by a postfocal transmittance minimum (valley) is observed in Figure 2(f). This is a signature of negative refractive nonlinearity, indicating that the Ph-C8-Ph chain shows a self-defocusing effect, as expected for most of the dispersive materials. Moreover, the nearly symmetrical profile with respect to the focal point satisfies the condition: $\Delta Z_{p-v} \sim 1.7 \cdot z_0$ where $z_0 = kw_0^2/2$ is the diffraction length of the beam; $k = 2\pi/\lambda$ is the wave vector; w_0 is the beam waist radius; and k is the laser wavelength. The occurrence of the above value confirms the presence of cubic nonlinearity and a small phase distortion.[23,39] In this case, the observed self-defocusing effect indicates that also the refractive index change contributes to determining the nature of the optical limiting response of the Ph-C8-Ph carbon chains.

A quantitative evaluation of the nonlinear absorption coefficient β and the refractive one can be carried out using the following procedure.[23] We outline that the absorptive and refractive contributions to the far-field beam profile and, hence, the Z-scan transmittance are coupled. When the aperture (S) is removed before the detector, the Z-scan transmittance is insensitive to beam distortion, and it is only a function of the nonlinear absorption. The total transmitted power $P(z, t)$ is given by

$$P(z, t) = P_i(t)e^{-\alpha L}\frac{I[1 + q_0(z, t)]}{q_0(z, t)} \quad (1)$$

where $\alpha(I)$ includes linear and nonlinear absorption terms; L is the sample length; and $q_0(z,t)$ is the parameter characterizing the strength of the nonlinearity given by the following expression: $q_0(z, t) = (\beta I_0(t))(L_{eff}/(1 + (z^2/z_0^2)))$ (z is the sample position; L_{eff} is the effective interaction length; z_0 is the Rayleigh diffraction length); $P_i(t)$ is the instantaneous input power defined as $P_i(t) = (\pi w_0^2 I_0(t)/2)$; and S is the aperture

dx.doi.org/10.1021/jp509666x | J. Phys. Chem. C 2014, 118, 28812−28819

linear transmittance given by $S = 1 - e^{[(-2r_a^2)/(w_0^2)]}$ with r_a denoting the beam radius at the aperture, in the linear regime.

For a temporally Gaussian pulse, the normalized energy transmittance is expressed by

$$T(z, S = 1) = \frac{1}{\sqrt{\pi}\, q_0(z, 0)} \cdot \int_{-\infty}^{+\infty} I[1 + q_0(z, 0)e^{-i\tau^2}]\mathrm{d}\tau \tag{2}$$

Moreover, for $|q_0| < 1$, this transmittance can be expressed in terms of the peak irradiance in a summation, more suitable for numerical evaluation

$$T(z, S = 1) = \sum_{m=0}^{\infty} \frac{[-q_0(z, 0)]^m}{(m + 1)^{3/2}} \tag{3}$$

Thus, for $S = 1$, fitting experimental data with this expression, the nonlinear absorption coefficient β was unambiguously deduced. With β known, the Z-scan with aperture $S < 1$ can be used to determine the coefficient n_2. In this case, the closed/open Z-scan transmittance can be reproduced considering a geometry-independent normalized transmittance as

$$T(z) \propto 1 - \frac{4x}{(x^2 + 9)\cdot(x^2 + 1)} \tag{4}$$

where $x = z/z_0$, while the peak and valley transmittance values are calculated by solving the equation: $(dT(z))/(dz) = 0$. Thus, the nonlinear refraction index n_2 value can be estimated using the relation

$$n_2 = \frac{\lambda}{2\pi L} \cdot \frac{\Delta T_{p-v}}{0.406(1 - S)^{0.25} I} \tag{5}$$

where λ is the laser wavelength, and S is the finite aperture parameter.

Finally, knowing β, the nonlinear scattering coefficient α_s was estimated taking into account that the transmitted intensity through the sample is given by

$$\frac{dI}{dz} = -\alpha_s I - \beta I^2 \tag{6}$$

The results of the fitting procedure are shown (solid lines) in Figure 3(a,b,c,d).

From the fitting results, the nonlinear absorption coefficient β values are found: 1.6×10^{-11} cm/W and -1.02×10^{-9} cm/W for Ph-C4-Ph and Ph-C8-Ph, respectively. The negative β sign is representative of a significant modification of the "symmetry" of the differently end-capped LCCs. Regarding the scattering coefficient and refractive index values, the Ph-C8-Ph estimated value of α_s is 5.38 cm^{-1}, while the n_2 value is negative and equal to -5.03×10^{-15} cm^2/W. At the focal point a local heating could have occurred, caused by the conversion of part of the absorbed energy into heat and then transferred to the liquid which, in turn, induces a local density reduction with a refractive index change.[23,39,40] Nevertheless, no microbubble formation in the solutions was observed, and the measurements, carried out even at a repetition frequency as low as 1 Hz, showed no significant change, pointing out that the thermal contribution (n_{2th}) to the nonlinear refractive index (n_2) is almost absent.

Moreover, during the nearly 1 h lasting experiment, no changes were observed in the Z-scan trace, suggesting a negligible degradation of the solution in the investigated conditions.

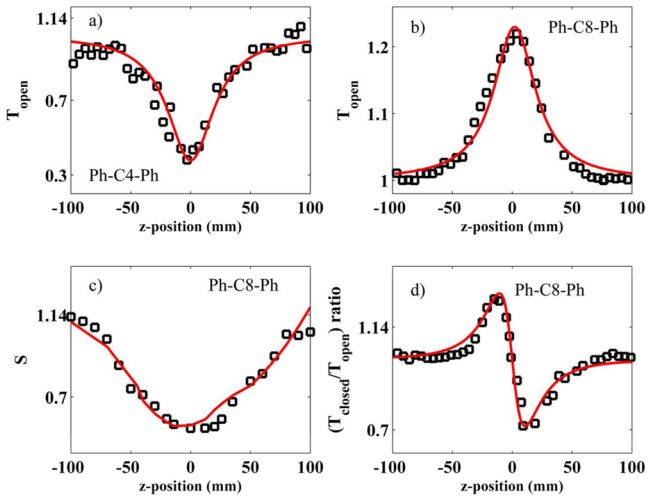

Figure 3. Experimental (open square) and fitted (solid line) Z-scan data. The values are normalized to the ones acquired outside the region of nonlinearity.

Finally, the estimated molecular second-order hyperpolarizability γ for the Ph-C4-Ph and Ph-C8-Ph samples is 1.7×10^{-31} esu and 1.3×10^{-30} esu, respectively. These values compare fairly well with those (ranging from nearly 10^{-33} esu to 3.5×10^{-29} esu) estimated for the β-carotene polymer, some hyperbranched polyynes,[41,42] and both armchair and single wall nanotubes,[36] which are considered good optical limiting carbon-based materials.

Only after several repeated cycles of measurements, a softening of the optical limiting response is observed, even if the effect is still active. Possible molecular structure modifications have been investigated by means of UV−vis optical absorption measurements, carried out after the optical limiting measurements, to test for the Ph-C*n*-Ph structure degradation.

4.2. UV−vis Absorption/Emission Spectra. In Figure 4(a,b,c) the UV−vis spectral data before and after the Z-scan measurements are shown. As can be observed in the as-prepared samples, we obtain spectra with two prominent absorption structures, both electronic features red-shifted as the number of carbon atoms/chains increases.

The position of the Ph-Cn-Ph electronic absorption peaks is correlated with the molecular weight and thus with the number of sp bonds. Previous studies associated the region at higher wavelength (280−340 nm for Ph-C4-Ph and 310−410 nm for Ph-C8-Ph) to electronic transitions between the highest occupied molecular orbital (HOMO) and the lowest unoccupied molecular orbital (LUMO), while the second region at lower wavelength, below 280 nm for Ph-C2-Ph and Ph-C4-Ph (see Figure 4(a) and Figure 4(b)) and lower than 310 nm for Ph-C8-Ph (see Figure 4(c)), was related to transitions between HOMO and LUMO+1 or the HOMO−1 and LUMO.[14] The presence in the higher wavelength region of multiple absorption peaks can be attributed both to the occurrence of HOMO−LUMO electronic transition and to the excitation of vibrational modes of the molecule involved in the same transition.[14] As shown in Figure 4 (b,c), the position of the peaks at 325 and 395 nm, respectively, for our Ph-C4-Ph and Ph-C8-Ph samples strongly matches with values reported by Cataldo et al.[14] for diphenyl polyynes. According to literature data, the 70 nm shift is associated with the decrease of the HOMO−LUMO gap, occurring at higher polyynic chain

dx.doi.org/10.1021/jp509666x | J. Phys. Chem. C 2014, 118, 28812−28819

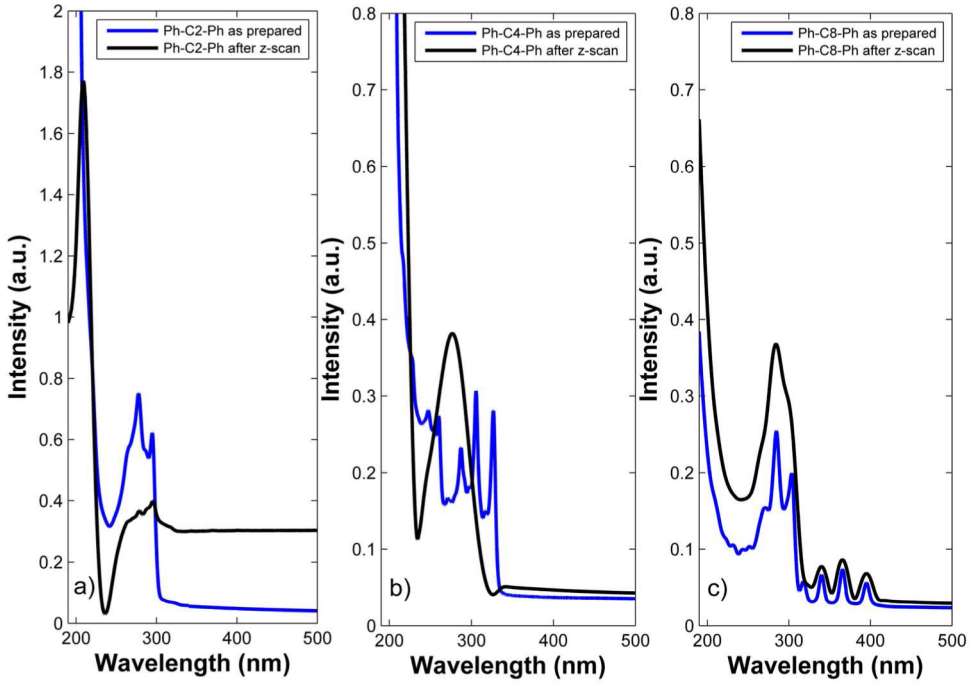

Figure 4. UV−vis absorption spectra for the Ph-C2-Ph (a), Ph-C4-Ph (b), and (c) Ph-C8-Ph carbon chains, before and after the Z-scan measurements.

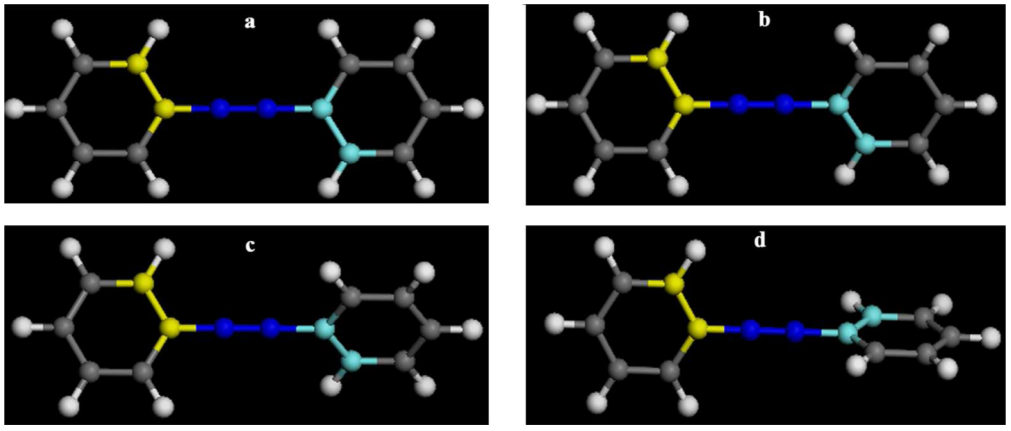

Figure 5. Upper four isomers of Ph-C2-Ph are shown. The carbon atoms colored in blue form a dihedral angle with the two carbon atoms colored in yellow of 0 (a), 30 (b), 60 (c), and 90 (d). The same values are considered for the dihedral angle formed by both blue and cyan colored carbon atoms. For the sake of clarity Ph-C4-Ph and Ph-C8-Ph are omitted.

length. Multiple absorption structures positioned in the range 200−280 nm (Ph-C4-Ph) and 240−330 nm (Ph-C8-Ph) and the shifts of about 60 nm toward higher wavelengths are again ascribed to the increased chain length.

After the Z-scan measurements performed at the laser fluence of 1.5 J/cm^2, the UV−vis absorption features typical of the Ph-C2-Ph and Ph-C4-Ph carbon chains are less visible or totally absent, and only a broad band in the 200−300 nm range centered at 280 nm can be observed. It is plausible that a degradation of the carbon molecules occurs, in part, by cross-linking reactions leading to the formation of sp^2-coordinated carbon species whose relative absorption contribution is indicated by the structureless increased background.

Moreover, we do not exclude the occurrence of reactions of hydroxylation and carboxylation of phenyl termination that could contribute both to the detection of the 280 nm broad band (Figure 4b,c) and to the disappearance of the aromatic features at 220 < λ < 270 nm.

It is well-known that conjugation effects of substituent groups in the phenyl termination with π-electrons of the aromatic ring can cause a red shift of the benzene absorption features. For the Ph-C8-Ph chains, we observed a similar trend in the 200−300 nm region of the absorption contributions. On the contrary, the three absorption features located at wavelengths greater than 300 nm are well-defined and nearly indistinguishable from that observed in the as-prepared samples.

4.3. DFT Calculations. An accurate computational study was carried out in order to discuss the transitions observed in the UV absorption spectra. In detail, the lowest energy structures, obtained after geometry optimization, are planar, as shown for the Ph-C2-Ph in Figure 5(a). The other Ph-C2-Ph isomers, with dihedral angle between the carbon chain and the

dx.doi.org/10.1021/jp509666x | J. Phys. Chem. C 2014, 118, 28812−28819

phenyl group of 30 (Figure 5(b)), 60 (Figure 5(c)), and 90 (Figure 5(d)), are also shown.

For the sake of clarity the four isomers of Ph-C4-Ph and Ph-C8-Ph are omitted; their optimized geometries are however reported in the Supporting Information.

Nevertheless, the energy differences among rotational isomers are quite small, as reported in Table 1. In the case of Ph-C2-Ph, the highest value of energy difference was found to amount to about 3 kJ/mol; such a result can be ascribed to the low flexibility of such a compound due to the short length of the linear chain. Indeed once the polyynic chain becomes longer the energy differences become negligible. This finding indicates that, basically, all the rotational isomers contribute to UV spectra; therefore, experimental data report the weighted average of such contributions.

Table 1. Energy Difference Values Are Reported Above in kJ/mol[a]

compound	ΔE (kJ/mol)	compound	ΔE (kJ/mol)
C-2-0	0	C-4-60	0.79
C-2-30	0.79	C-4-90	1.05
C-2-0	2.89	C-8-0	0
C-2-90	3.68	C-8-30	0.03
C-4-0	0	C-8-60	0.24
C-4-30	0.26	C-8-90	0.26

[a]Planar structures (0°) show the minimum value and are taken as a reference.

Moreover, polarizability volume α values calculated for isomers C-n-0 and C-n-90 (n = 2,4,8) suggest that the electronic distribution in planar geometries is more responsive to the effect of an electric field for longer chains, and the major contribution to α is found along the direction parallel to the linear chain (see Table 2).

Table 2. Polarizability Volumes α Reported in Bohr^3 for Linear and T Conformers

compound	α (Bohr^3)
C-2-0	184.28
C-2-90	175.73
C-4-0	238.89
C-4-90	230.92
C-8-0	388.18
C-8-90	381.62

This result is in agreement with the below reported UV−vis data analysis, showing that the longer linear chain conformers easily overcome the rotational barrier converting each other.

Turning toward UV electronic transition analysis we preliminarily observe that:

(i) comparison among compounds with different CC chain length highlights how the increase of the linear chain affects the HOMO → LUMO transition causing both a higher wavelength shift and an intensity decrease. Conversely the HOMO−1 → LUMO+1 transition increases in intensity but undergoes a bathochromic shift (see Supporting Information, Table SI.1);

(ii) comparison among isomers points out that a larger dihedral angle gives rise to a blue shift and an intensity reduction of the HOMO → LUMO transition. Finally the HOMO−1 → LUMO+1 transition shows the opposite trend with respect to the HOMO → LUMO.

That said we have compared calculated and experimental UV spectra with the aim of assigning the various transitions of the studied compounds (see Figure 6(a,b,c)). As far as Ph-C2-Ph is concerned, the observed transitions between 275 and 300 nm (see Figure 6(a)) can be attributed to the HOMO → LUMO transition of C-1-0, C-1-30, and C-1-60 (see Table SI.1, Supporting Information); in more details from Figure SI.2 (see Supporting Information), we learn that for C-1-0 and C-1-30 the HOMO concerns the whole molecule, while LUMO shows a strong aromatic peculiarity. Such a finding suggests that such transitions are due to the aromatic moieties of the molecules.

The increase of the CC length gives rise to a broader π-delocalization, and therefore further transitions take place. As shown in Figure 6(b), the experimental absorption band of Ph-C4-Ph dispersions, observed at around 326 nm, is attributed to a HOMO → LUMO transition; however, in this case, both MOs are extended to the whole molecule, and a prominent role is played by C-2-30 and C-2-60. Such a finding confirms that conformers freely convert each other, overcoming rotational barrier. In other words, experimental UV transitions account for several stable conformers, arising from rotation of aromatic groups.

Finally, considering Ph-C8-Ph, we have found that bands occurring in the range between 340 and 400 nm (see Figure 6(c)) are mainly due to HOMO−1 → LUMO+1 transitions. Therefore, on the basis of calculated and experimentally recorded spectra, conjugation in a linear chain plays a significant role in these electronic transitions. Moreover it is worth noting that HOMO → LUMO transitions occurring at about 475 nm for C-4-0 and C-4-30, respectively, indicate that planar (and nearly planar) structures give a negligible contribution when the transition HOMO → LUMO is considered (see Table SI.I in the Supporting Information).

The interesting link between the effects determined by the increase of the number of carbon atoms in the chains (chain

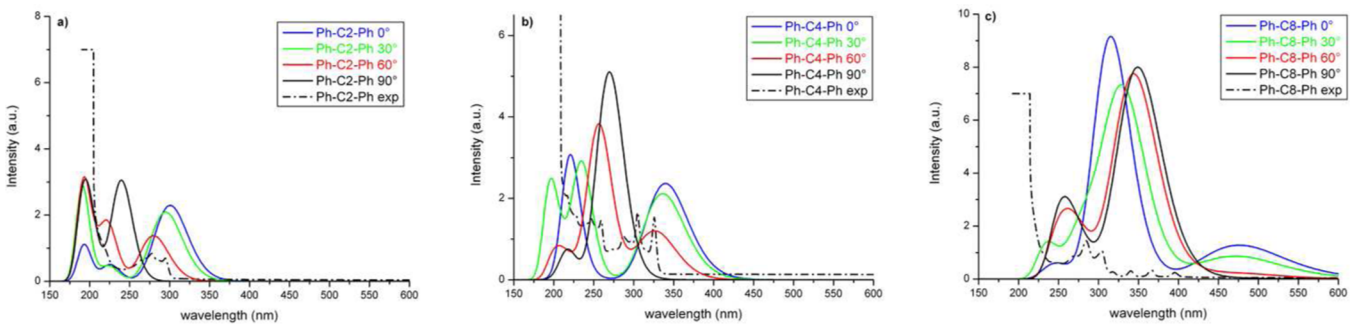

Figure 6. Comparison between calculated and experimental UV are reported for Ph-C2-Ph (a), Ph-C4-Ph (b), and Ph-C8-Ph (c).

dx.doi.org/10.1021/jp509666x | J. Phys. Chem. C 2014, 118, 28812−28819

deformations and higher polarizability) and the optoelectronic behavior is also confirmed by the observations reported by Nagano et al.[18] on the symmetry switching of the fluorescent excited state in diphenylpolyynes. According to their results, the multiple bond number dependence of the oscillator strength (f) of the first adsorption band becomes smaller with the increase of the triple-bond number. Such a finding is in agreement with our calculated transitions (see Table SI.1 in the Supporting Information); as to the value of f, one can expect a lower nonlinear response of Ph-C8-Ph, as we have found, with respect to the shorter Ph-C4-Ph and Ph-C2-Ph. In fact a large value of the oscillator strength in the shortest transition f is strictly associated with an enhancement of the nonlinear response.

On the other hand, the linear optical properties of phenyl-terminated polyynes and the correlation with the torsional stiffness were already highlighted by Ravagnan et al.[19] whereby studies were carried out on the correlation between axial torsion and electronic transitions in sp^2-terminated carbon chains. They reported for these molecules a non-negligible bond-length alternation (BLA), with respect to the traditional categories of polyynes (alternating single−triple bonds, yielding a large BLA) and cumulenes (double bonds, negligible BLA). Given the short length of the linear chain, the Ph-C2-Ph shows low flexibility, while upon increasing the CC length, the conformers freely convert each other, overcoming the rotational barrier. The rotation of aromatic groups affects BLA, determining a broader π-delocalization. Moreover, we have seen that a HOMO transition concerns the whole molecule, while the LUMO transition shows a strong aromatic peculiarity. Overall, the aromatic moieties of the molecules as well as the chain lengths and the orientation of the chains bonded to the sp^2-terminated structures are responsible for the change observed in the optical properties. As discussed in the paper of Ravagnan et al.,[19] the BLA of the sp^2-terminated chains varies substantially with the nature of the termination itself, being minimal in the case of a simple CH_2 termination but increasing substantially in diphenyl-terminated chains. Indeed, a memory of the orientation of the bonds of the terminating sp^2 carbon propagates along the sp-hybridized chain, so that even-n chains tend to relax to a configuration where the termination sp^2 planes coincide while odd-n chains tend to keep their terminations at the twist angle of 90°. So, despite their purely one-dimensional nature, sp^2-terminated carbon chains display a nonvanishing torsional stiffness.[19]

In addition to singlet transitions, Fazzi et al.[43] reported an intersystem crossing event, leading to the formation of triplet excited states, on dinapthylpolyynes characterized by four triple bonds in the chain.

In light of the above results, and being well-known that triplet states are responsible for nonlinear absorption,[44] triplet−triplet transitions were also evaluated for the Ph-C8-Ph conformers by DFT calculation. The main transitions involve molecular orbitals having both aromatic and polyynic features. In detail, all the bands are red-shifted, compared to the singlet state, and aromatic bands disappear. On the other hand, absorptions between 538 and 580 nm, with considerable values (about 1.5) of the oscillator strength, occur involving the HOMO → LUMO+1 transition.

5. CONCLUSION

A high optical nonlinear response of monodispersed diphenylpolyyne has been reported. The experimental evidence indicates that molecular arrangement of these molecules strongly influences their chemical and optoelectronic properties. In view of the observed scattering phenomena involving the longer carbon molecules, we hypothesize that a pronounced photoinduced molecular reorientation takes place at higher energy density (focal region), and the alignment of the molecules leads to a decrease of the scattering phenomena, thus influencing the nonlinear optical behavior of carbon nanowires. Further, the good optical transparency in the visible region and the relatively good photostability of the investigated carbon chains make them interesting materials for potential applications in the nonlinear optics field as well as base materials for photonic devices and multiphoton fluorescence imaging applications.

■ ASSOCIATED CONTENT

Supporting Information

Detailed experimental procedures on the synthesis and characterization of monodispersed diphenylpolyynes, equilibrium geometries of Ph-Cn-Ph (n = 2,4,8) by DFT calculations, and table of diphenylpolyyne electronic transitions. This material is available free of charge via the Internet at http://pubs.acs.org.

■ AUTHOR INFORMATION

Corresponding Author

*Telephone number: +39 095 7385129. Fax: +39 095 580138. E-mail: ldurso@unict.it (L. D'Urso).

Notes

The authors declare no competing financial interest.

■ ACKNOWLEDGMENTS

The authors wish to thank the Consorzio Interuniversitario Cineca for the computational support and Dr. Alessandro Ridolfo and Prof. R. Saija of Messina University for fruitful discussions about the implementation of the fitting procedure and the results interpretation. The authors gratefully acknowledge the project PON R&C 2007-2013 (PON02 00355), funded by Ministero Istruzione Università e Ricerca.

■ REFERENCES

(1) Sunjoo Kim, F.; Ren, G.; Jenekhe, S. A. One-Dimensional Nanostructures of π-Conjugated Molecular Systems: Assembly, Properties, and Applications from Photovoltaics, Sensors, and Nanophotonics to Nanoelectronics. *Chem. Mater.* **2011**, *23*, 682−732.

(2) Liu, M.; Artyukhov, V. I.; Lee, H.; X, u F.; Yakobson, B. I. Carbyne from First Principles: Chain of C Atoms, a Nanorod or a Nanorope. *ACS Nano* **2013**, *7*, 10075−10082.

(3) Arakawa, Y.; Kang, S.; Nakajima, S.; Sakajiri, K.; Cho, Y.; Kawauchi, S.; Watanabe, J.; Konishi, G. Diphenyltriacetylenes: Novel Nematic Liquid Crystal Materials and Analysis of their Nematic Phase-Transition and Birefringence Behaviours. *Mater. Chem. C* **2013**, *1*, 8094.

(4) Milani, A.; Lucotti, A.; Russo, V.; Tommasini, M.; Cataldo, F.; Li Bassi, A.; Casari, C. S. Charge Transfer and Vibrational Structure of sp-Hybridized Carbon Atomic Wires Probed by Surface Enhanced Raman Spectroscopy. *J. Phys. Chem. C* **2011**, *115*, 12836−12843.

(5) Wakabayashi, T.; Nagayama, H.; Daigoku, K.; Kiyooka, Y.; Hashimoto, K. Laser Induced Emission Spectra of Polyyne Molecules $C_{2n}H_2$ (n = 5−8). *Chem. Phys. Lett.* **2007**, *446*, 65−70.

(6) D'Urso, L.; Compagnini, G.; Puglisi, O.; Scandurra, A.; Cataliotti, R. S. Vibrational and Photoelectron Investigation of Amorphous Fluorinate Carbon Films. *J. Phys. Chem. C* **2007**, *111*, 17437−17441.

(7) Kavan, L.; Dousek, F. P.; Micka, K. Time-dependent Electrical Resistivity of Carbon. *J. Phys. Chem.* **1990**, *94*, 5127−5134.

(8) Kavan, L.; Dousek, F. P. Carbynoid Species in Electrochemical Polymeric Carbon. *Synth. Met.* **1993**, *58*, 63−72.

(9) Kastner, J.; Kuzmany, H.; Kavan, L.; Dousek, F. P.; Kurti, J. Reductive Preparation of Carbine with High Yield. An in Situ Scattering Study. *Macromolecules* **1995**, *28*, 344−353.
(10) Grasso, G.; D'Urso, L.; Messina, E.; Cataldo, F.; Puglisi, O.; Spoto, G.; Compagnini, G. A Mass Spectrometry and Surface Enhanced Raman Spectroscopy Study of the Interaction Between Linear Carbon Chains and Noble Metals. *Carbon* **2009**, *47*, 2611−2619.
(11) Zhao, X.; Ando, Y.; Liu, Y.; Jinno, M.; Suzuki, T. Carbon Nanowire Made of a Long Linear Carbon Chain Inserted Inside a Multiwalled Carbon Nanotube. *Phys. Rev. Lett.* **2003**, *90*, 187401−187404.
(12) Scalese, S.; Scuderi, V.; Bagiante, S.; Simone, F.; Russo, P.; D'Urso, L. Controlled Synthesis of Carbon Nanotubes and Linear C Chains by Arc Discharge in Liquid Nitrogen. *J. Appl. Phys.* **2010**, *107*, 014304−014306.
(13) Sugiyama, J.; Tomita, I. Novel Approach to Stabilize Unstable Molecular Wires by Simultaneous Rotaxane Formation − Synthesis of Inclusion Complexes of Oligocarbynes with Cyclic Host Molecules. *Eur. J. Org. Chem.* **2007**, *28*, 4651−4653.
(14) Cataldo, F.; Ravagnan, L.; Cinquanta, E.; Castelli, I. E.; Manini, N.; Onida, G.; Milani, P. Synthesis, Characterization, and Modeling of Naphthyl-Terminated sp Carbon Chains: Dinaphthylpolyynes. *J. Phys. Chem. B* **2010**, *114*, 14834−14841.
(15) Cataldo, F.; Ursini, O.; Angelini, G.; Tommasini, M.; Casari, C. Simple Synthesis of α, ω-Diarylpolyynes Part 1:Diphenylpolyynes. *J. Macromol. Sci., Part A: Pure Appl. Chem.* **2010**, *47*, 739−746.
(16) Luu, T.; Elliott, E.; Slepkov, A. D.; Eisler, S.; McDonald, R.; Hegmann, F. A.; et al. Synthesis, Structure, and Nonlinear Optical Properties of Diarylpolyynes. *Org. Lett.* **2005**, *7*, 51−54.
(17) Chalifoux, W.; Tykwinski, R. Synthesis of Polyynes to Model the sp-Carbon Allotrope Carbyne. *Nat. Chem.* **2010**, *2*, 967−971.
(18) Nagano, Y.; Ikoma, T.; Akiyama, K.; Tero-Kubota, S. Symmetry Switching of the Fluorescent Excited State in α,ω-Diphenylpolyynes. *J. Am. Chem. Soc.* **2003**, *125*, 14103−14112.
(19) Ravagnan, L.; Manini, N.; Cinquanta, E.; Onida, G.; Sangalli, D.; Motta, C.; Devetta, M.; Bordoni, A.; Piseri, P.; Milani, P. Effect of Axial Torsion on sp Carbon Atomic Wires. *Phys. Rev. Lett.* **2009**, *102*, 245502.
(20) Pati, A. K.; Gharpure, S. J.; Mishra, A. K. Substituted Diphenyl Butadiynes: a Computational Study of Geometries and Electronic Transitions Using DFT/TD-DFT†. *Phys. Chem. Chem. Phys.* **2014**, *16*, 14015−14028.
(21) Forte, G.; D'Urso, L.; Fazio, E.; Patanè, S.; Neri, F.; Puglisi, O.; Compagnini, G. The Effects of Liquid Environments on the Optical Properties of Linear Carbon Chains Prepared by Laser Ablation Generated Plasmas. *Appl. Surf. Sci.* **2013**, *272*, 76−81.
(22) Liu, Q.; Burton, D. J. A Facile Synthesis of Diynes. *Tetrahedron Lett.* **1997**, *38*, 4371−4374.
(23) Sheik-Bahae, M.; Said, A. A.; Wei, T.; Hagan, D. J.; Van Stryland, E. W. Sensitive Measurement of Optical Nonlinearities Using a Single Beam. *IEEE J. Quantum Electron.* **1990**, *26*, 760−769.
(24) Perdew, J. P.; Burke, K.; Ernzerhof, M. Generalized Gradient Approximation Made Simple. *Phys. Rev. Lett.* **1996**, *77*, 3865−3868.
(25) Perdew, J. P.; Burke, K.; Ernzerhof, M. Errata: Generalized Gradient Approximation Made *Simple*. *Phys. Rev. Lett.* **1997**, *78*, 1396−1396.
(26) Adamo, C.; Barone, V. Toward Reliable Density Functional Methods Without Adjustable Parameters: The PBE0Model. *J. Chem. Phys.* **1999**, *110*, 6158−6169.
(27) McLean, A. D.; Chandler, G. S. Contracted Gaussian Basis Sets for Molecular Calculations. I. Second Rowatoms, Z = 11−18. *J. Chem. Phys.* **1980**, *72*, 5639−5648.
(28) Krishnan, R.; Binkley, J. S.; Seeger, R.; Pople, J. A. Self-Consistent Orbital Methods. XX. A Basis Set for Correlated Wave Functions. *J. Chem. Phys.* **1980**, *72*, 650−654.
(29) Klamt, A.; Schüürmann, G. COSMO a New Approach to Dielectric Screening in Solvents with Explicit Expressions for the Screening Energy and its Gradient. *J. Chem. Soc., Perkin Trans.* **1993**, *2*, 799−805.
(30) Cossi, M.; Rega, N.; Scalmani, G.; Barone, V. Energies, Structures, and Electronic Properties of Molecules in Solution with the C-PCM Solvation Model. *J. Comput. Chem.* **2003**, *24*, 669−681.
(31) Takano, Y.; Houk, K. N. Benchmarking the Conductor-Like Polarizable Continuum Model (CPCM) for Aqueous Solvation Free Energies of Neutral and Ionic Organic Molecules. *J. Chem. Theor. Comput.* **2005**, *1*, 70−77.
(32) Runge, E.; Gross, E. K. U. Density-Functional Theory for Time-Dependent Systems. *Phys. Rev. Lett.* **1984**, *52*, 997−1000.
(33) Hohenberg, P.; Kohn, W. Inhomogeneous Electron Gas. *Phys. Rev.* **1964**, *136*, B864−B871.
(34) Casida, M. E.; Jamorski, C.; Bohr, F.; Guan, J.; Salahub, D. R. *Theoretical and Computational Modeling of NLO and Electronic Materials*; Karna, S. P., Yeates, A. T., Eds.; ACS Press: Washington, D.C., 1996; p 145.
(35) Xie, R. H.; Rao, Q. A Scaling Law of the Second-Order Hyperpolarizability in Armchair Nanotube. *Appl. Phys. Lett.* **1998**, *72*, 2358−2360.
(36) Seo, J.; Ma, S.; Yang, Q.; Creekmore, L.; Battle, R.; Tabibi, M.; Brown, H.; Jackson, A.; Skyles, T.; Tabibi, B. Third-order Optical Nonlinearities of Singlewall Carbon Nanotubes for Nonlinear Transmission Limiting Application. *J. Phys. Conf. Ser.* **2006**, *38*, 37−40.
(37) Sakai1, H.; Safvan, C. P.; Larsen, J. J.; Hilligso/e, K. M.; Hald, K.; Stapelfeldt, H. Controlling the Alignment of Neutral Molecules by a Strong Laser Field. *J. Chem. Phys.* **1999**, *110*, 10235−10238.
(38) Borghese, F.; Denti, P.; Saija, R.; Iatì, M. A.; Maragò, O. M. Radiation Torque and Force on Optically Trapped Linear Nanostructures. *Phys. Rev. Lett.* **2008**, *100*, 163903−1−4.
(39) Fazio, E.; Neri, F.; Patanè, S.; D'Urso, L.; Compagnini, G. Optical Limiting Effects in Linear Carbon Chains. *Carbon* **2011**, *49*, 306−310.
(40) Shen, R. *The Principles of Nonlinear Optics*; Wiley: New York, 1984; p 202.
(41) Castro-Beltran, R.; Ramos-Ortiz, G.; Jim, C. K. W.; Maldonado, J. L.; Haubler, M.; Dominguez, D. P. Optical Nonlinearities in Hyperbranched Polyyne Studied by Two-Photon Excited Fluorescence and Third-Harmonic Generation Spectroscopy. *Appl. Phys. B: Laser Opt.* **2009**, *97*, 489−496.
(42) Slepkov, A. D.; Hegmann, F. A.; Eisler, S.; Elliott, E.; Tykwinski, R. R. The Surprising Nonlinear Optical Properties of Conjugated Polyyne Oligomers. *J. Chem. Phys.* **2004**, *120*, 6807−6810.
(43) Fazzi, D.; Scotognella, F.; Milani, A.; Brida, D.; Manzoni, C.; Cinquanta, E.; Devetta, M.; Ravagnan, L.; Milani, P.; et al. Ultrafast Spectroscopy of Linear Carbon Chains: the Case of Dinaphthylpolyynes. *Phys. Chem. Chem. Phys.* **2013**, *15*, 9384−9391.
(44) Perry, J. W.; Mansour, K.; Lee, I. Y. S.; Wu, X. L.; Bedworth, P. V.; Chen, C. T.; Marder, S. R.; Miles, P.; Wada, T.; Tian, M.; et al. Organic Optical Limiter with a Strong Nonlinear Absorptive Response. *Science* **1996**, *273*, 1533−1536.